



# High-performance thermotropic starch-based liquid crystalline polymer

Wenyi Huang<sup>a,\*</sup>, Er Shi<sup>b</sup>

<sup>a</sup> Department of Polymer Engineering, The University of Akron, 250 South Forge Street, Akron, OH 44325-0301, USA

<sup>b</sup> School of Energy and Power Engineering, Changsha University of Technology and Science, Changsha 410076, China

## ARTICLE INFO

### Article history:

Received 16 February 2012

Received in revised form 21 April 2012

Accepted 11 May 2012

Available online 6 June 2012

### Keywords:

Liquid-crystalline polymers (LCP)

Starch

Differential scanning calorimetry (DSC)

Mechanical properties

Synthesis

## ABSTRACT

A thermotropic starch liquid crystalline polymer (St-10CN) was successfully synthesized by high-degree substitution (esterification) of the hydroxyl groups resided on the starch with mesogenic 11-(4'-cyano-biphenyl-4-yloxy)-undecanoic chloride in the presence of pyridine. The degree of substitution of St-10CN was calculated to be 2.68 based on the result of elemental analysis. The chemical structure of the polymer was confirmed using Fourier transfer infrared (FTIR) spectroscopy and nuclear magnetic resonance spectroscopy. The thermal transitions of St-10CN were determined using differential scanning calorimetry and its mesophase structures were characterized using polarized optical microscopy (POM) and wide-angle X-ray diffraction (WAXD). This unique starch-based side-chain liquid crystalline polymer is glassy and smectic with excellent thermal stability, and has tensile strength of  $37.9 \pm 7.0$  MPa and Young's modulus of  $1.42 \pm 0.14$  GPa.

Published by Elsevier Ltd.

## 1. Introduction

In recent years, tremendous efforts have been devoted to develop sustainable polymers based on renewable raw materials like cellulose and starch, which are abundant and biodegradable (Carvalho, 2008; Liu, Xie, Yu, Chen, & Li, 2009). Nevertheless, pure starch itself is so hydrophilic, viscous, and brittle that it cannot be considered as a thermoplastic and only has limited applications. One approach to make thermoplastic starch is to process it in the presence of low-molecular-weight plasticizers like water, glycerol, sorbitol, and so on, which has been widely employed in the commercially compostable products, but at the same time causes a lot of troubles like poor water resistance and inferior mechanical properties (Greer, 2006). Another approach to obtain thermoplastic starch is chemical modification, because starch molecules possess three hydroxyl groups per repeated unit, which exhibit high reactivity with a plethora of functional groups and thus open an effective pathway toward practical utilization through a variety of strategies, such as grafting polymerization (Choi, Kim, & Park, 1999; Dubois, Krishnan, & Narayan, 1999), nitration (Israelashvili, 1950; Tomasik & Schilling, 2004), etherification (Petzold, Klemm, Stein, & Günther, 2002; Trimmell, Stout, Doane, & Russell, 1978), and esterification (Grote & Heinze, 2005; Yang & Montgomery, 2006). Among these, starch esters are of special interest because high degree of substitution can be easily achieved under certain reaction conditions, and more importantly, the introduction of hydrophobic side chains into

starch molecules can significantly interrupt the hydrogen bonding between the hydroxyl groups of starch as well as destroy the granular semicrystalline structure of natural starch. As a result, the glass transition temperature and the melting temperature of starch, along with its hydrophilicity, would be dramatically reduced, and thus it could perform like thermoplastic materials (Aburto et al., 1997, 1999; Neumann, Wiege, & Warwel, 2002; Thiebaud et al., 1997).

Since the amylopectin molecule in starch is highly branched and its side chain branches are known to form double helices, the rigid entities with long persistence lengths, the concept of side-chain liquid crystalline polymer has been borrowed to interpret the structures and physical properties of starch (Daniels & Donald, 2004; Waigh, Perry, Riekel, Gidley, & Donald, 1998; Waigh, Gidley, Komanshek, & Donald, 2000; Waigh, Kato, Donald, Gidley, et al., 2000). However, it is impossible to observe thermotropic liquid crystalline behaviors in native starch because its melting temperature and glass transition temperature are well above its thermal degradation temperature. In contrast, cellulose and its derivatives are well-known to exhibit mesophases in either lyotropic or thermotropic states (Chen, Huang, Yuan, Yan, & Ye, 1992; Shaikh, Maldar, Lonikar, Rajan, & Ponrathnam, 1999; Werbowyj & Gray, 1976), and more recently side-chain mesogenic units were attached onto cellulose to form combined main-chain/side-chain thermotropic liquid crystalline polymers (Hu, Yi, Xiao, & Zhang, 2010). Although starch has a similar chemical structure to cellulose, starch cannot form a liquid crystalline molecular order in the lyotropic state either, due to the fact that the amylopectin component is highly and multiply branched while both amylose and amylopectin have strong tendency to form complex aggregates

\* Corresponding author. Tel.: +1 330 622 3807; fax: +1 330 972 3406.

E-mail address: [polymerhuang@yahoo.com](mailto:polymerhuang@yahoo.com) (W. Huang).

**Table 1**  
<sup>1</sup>H and <sup>13</sup>C NMR (300 MHz, DMSO) data of 10CN-COOH.

Chemical shift $\delta$ in ppm	
$\delta_H$	$\delta_C$
1.18–1.55 (m, 14H, $-\text{CH}_2-$ )	24.5 ( $-\text{CH}_2-$ )
1.67 (s, 2H, $-\text{CH}_2-$ )	25.5 ( $-\text{CH}_2-$ )
2.17 (t, $J = 5.4$ Hz, 2H, $-\text{CH}_2-$ )	28.8 ( $-\text{CH}_2-$ )
4.00 (t, $J = 4.5$ Hz, 2H, $-\text{CH}_2\text{O}-$ )	33.6 ( $-\text{CH}_2-$ )
7.05 (d, $J = 8.7$ Hz, 2H, Ar-H)	67.6 ( $-\text{CH}_2\text{O}-$ )
7.70 (d, $J = 8.7$ Hz, 2H, Ar-H)	109.1 (Ar-C)
7.84 (d, $J = 4.8$ Hz, 4H, Ar-H)	115.1 ( $-\text{CN}$ )
11.95 (s, 1H, $-\text{COOH}$ )	126.8 (Ar-C)
	128.3 (Ar-C)
	130.2 (Ar-C)
	132.7 (Ar-C)
	144.3 (Ar-C)
	159.3 (Ar-C)
	174.5 ( $-\text{CO}-$ )

(Huber, Kaplan, & Viney, 1994). It is well-known that liquid crystalline polymers have excellent mechanical properties, dimensional stability, thermal stability coupled with the absence of creep and shrinkage; thus they are ideal candidates for high-performance applications (Donald & Windle, 1992). In this study, we present the synthesis and characterizations of a thermotropic starch liquid crystalline polymer (denoted by St-10CN) by high-degree esterification of mesogenic molecules with the hydroxyl groups resided on the starch. A long flexible spacer was judiciously incorporated into this mesogenic molecule to ensure that the clearing temperature of this polymer is well below its thermal degradation temperature. The presence of mesogenic units in starch liquid crystalline polymer greatly improves the mechanical properties of starch. Because of this, this starch-based biopolymer alone can find into a variety of applications such as plastic sheets and injection-molded parts.

## 2. Materials and methods

### 2.1. Materials

All reagents and solvents were purchased from Aldrich Chemical Company and used as received, if not otherwise mentioned. Acetone and pyridine were dried over calcium hydride and freshly distilled before use.

### 2.2. Synthesis of 11-(4'-cyano-biphenyl-4-yloxy)-undecanoic acid (10CN-COOH)

4'-Hydroxy-biphenyl-4-carbonitrile (10.3 g, 50 mmol) and anhydrous powdered potassium carbonate (20.7 g, 150 mmol) were dissolved in 80 mL of dry acetone. The reaction mixture was stirred at room temperature for 1 h under an argon gas atmosphere. After the temperature was raised to 50 °C, 11-bromo-undecanoic acid (14.6 g, 55 mmol) and a trace of potassium iodide in 50 mL of dry acetone were added dropwise into 4'-hydroxy-biphenyl-4-carbonitrile solution. The reaction mixture was heated to 60 °C and maintained for 4 days, and then acidified with 3 M HCl aqueous solution to make pH value less than 7 and diluted with 500 mL of distilled water. After filtration, the crude product was recrystallized from ethanol to obtain 10.4 g of final product. Yield: 55%. The chemical structure of 10CN-COOH was characterized by <sup>1</sup>H and <sup>13</sup>C NMR spectroscopy, the data of which were summarized in Table 1.

### 2.3. Synthesis of thermotropic starch liquid crystalline polymer (St-10CN)

To 11-(4'-cyano-biphenyl-4-yloxy)-undecanoic acid (7.6 g, 20 mmol) in 30 mL benzene was added 20 mL thionyl chloride and a few drops of N,N-dimethylformamide. The reaction mixture was heated to reflux for 5 h, and then cooled down to room temperature. The solvent was removed in vacuo to offer a yellow solid. The starch was dried at 100 °C for 24 h before reaction to avoid the interference of moisture. Corn starch (0.65 g) and 11-(4'-cyano-biphenyl-4-yloxy)-undecanoic chloride were placed in a 500 mL three-neck flask under an argon gas atmosphere, and then 80 mL of pyridine was added and heated to 100 °C for 24 h. Upon completion of the reaction, reaction mixture was diluted with 50 mL chloroform and filtered off to remove the insoluble fraction and the collected solution was concentrated under reduced pressure and then precipitated in 500 mL of ethanol. After filtration, the crude product was purified three times by dissolving in 30 mL chloroform and then precipitating in 200 mL ethanol to give 3.2 g yellowish powder, which was dried in vacuo at 60 °C for 3 days. Yield: 65%.

### 2.4. Nuclear magnetic resonance spectroscopy

<sup>1</sup>H NMR and <sup>13</sup>C nuclear magnetic resonance (NMR) spectra were measured on a Varian Mercury 300 spectrometer at 298 K. Chemical shifts ( $\delta$ ) were reported in ppm relative to the signal of tetramethylsilane (TMS). Residual solvent signals in the <sup>1</sup>H and <sup>13</sup>C NMR spectra were used as an internal reference. Coupling constants ( $J$ ) were given in Hz. The apparent resonance multiplicity was described as s (singlet), br s (broad singlet), d (doublet), t (triplet), q (quartet), and m (multiplet).

### 2.5. Fourier transform infrared spectroscopy

Fourier transform infrared (FTIR) spectra were recorded on a Thermo Nicolet 380 FTIR spectrometer (Thermo Fisher Scientific) with a diamond attenuated total reflectance (ATR) accessory. Thin films suitable for FTIR spectroscopy were prepared by casting 2% (w/v) solution in chloroform directly on the KBr salt plate. Film specimens were slowly dried for 24 h in a fume hood until most of the solvent evaporated and then dried at 80 °C in a vacuum oven.

### 2.6. Elemental analysis

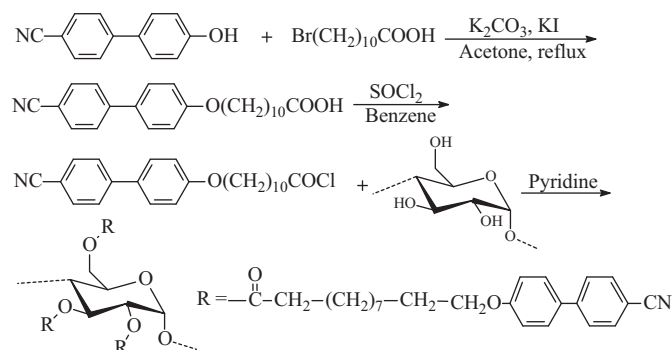
Elemental analyses were carried out in-house with an automatic analyzer LECO CHNS 932.

### 2.7. Differential scanning calorimetry

The thermal transition temperatures of the mesogenic molecule and polymer synthesized were determined by differential scanning calorimetry (DSC) (TA 200, TA Instrument). All DSC runs were made under a nitrogen atmosphere with heating and cooling rates of 10 °C/min. Indium and zinc were used to calibrate the temperature and heat of fusion.

### 2.8. Thermogravimetric analysis

The thermal degradation temperature of the polymer was determined by a thermogravimetric analyzer (TGA 2050, TA Instrument). All TGA data were measured under a nitrogen atmosphere at a heating rate of 10 °C/min, and the thermal degradation temperature was determined at the point of 95 wt% of the original weight.



**Scheme 1.** Reaction route for synthesizing a thermotropic starch liquid crystalline polymer (St-10CN).

### 2.9. Polarized optical microscopy

Polarized optical microscopy (POM) was used to observe the textures of the samples under cross-polarized light by using a Leitz Laborlux 12 Pol S polarized optical microscope equipped with a hot stage (Instec) and a digital camera (Spot insight 2, Diagnostic Instrument Inc.). Specimens were cast from 1 wt% solution of the polymer on a slide glass to obtain a film of about 2–3  $\mu$ m in thickness, which was initially dried in a fume hood and then in a vacuum oven. The heating and cooling rates used were 3  $^{\circ}$ C/min. Images of POM were obtained after keeping a specimen at a preset temperature for at least 10 min.

### 2.10. X-ray diffraction patterns

A Bruker X-ray generator operated at 40 kV and 150 mA was employed to determine the mesophase of the polymer. Wide-angle X-ray pattern image was recorded in General Electric X-ray generator (Model XRD-6) operated at 30 kV and 30 mA (Ni-filtered Cu K $\alpha$  radiation). Samples suitable for XRD measurement were prepared by solution casting into sheets of 2 mm, and then dried at 80  $^{\circ}$ C for 2 days in a vacuum oven.

### 2.11. Mechanical properties

The mechanical properties of starch liquid crystalline polymers were measured on an Instron tensile tester (Model 5567), according to ASTM (D 638-00) with a cross-head speed of 5 mm/min. The upper yield stress on the stress-strain curve was taken as the tensile strength of the specimens. Five measurements were conducted for each sample, and the results were averaged. Samples were prepared by compression molding at 170  $^{\circ}$ C.

## 3. Results and discussion

### 3.1. Characterizations of mesogenic monomer

The synthetic strategy to obtain starch liquid crystalline polymer (LCP) is depicted in Scheme 1. The mesogenic monomer, 11-(4'-cyano-biphenyl-4-yloxy)-undecanoic acid (10CN-COOH), was synthesized by reacting 4'-hydroxy-biphenyl-4-carbonitrile with 11-bromo-undecanoic acid in the presence of potassium carbonate and a catalytic amount of potassium iodide. Fig. S1 in the Supplementary Materials gives the polarized optical microscopy (POM) images of 10CN-COOH during the heating and cooling cycles. Upon heating, the initial crystalline structure at room temperature was transformed into smectic mesophase (image taken at 90  $^{\circ}$ C); then, Schlieren texture appears at 118  $^{\circ}$ C, which indicates the existence of nematic phase; finally, the

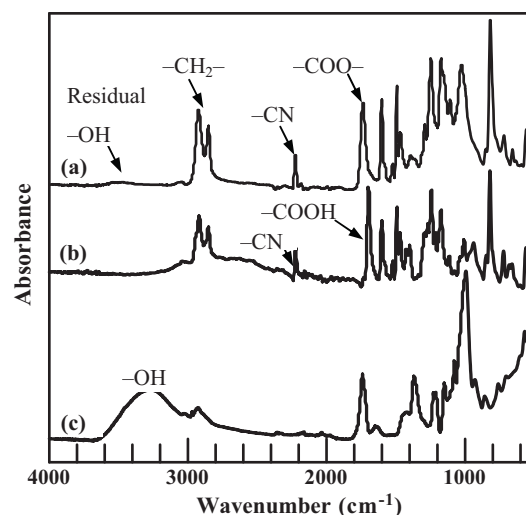


**Fig. 1.** FTIR spectra of (a) St-10CN, (b) 10CN-COOH, and (c) starch.

isotropic phase occurs at 130  $^{\circ}$ C. Upon cooling, nematic phase firstly appears at 100  $^{\circ}$ C (Schlieren texture), then smectic A mesophase (needle-like texture) exists at 0  $^{\circ}$ C, and consequently crystalline structure reappears at 30  $^{\circ}$ C. Accordingly, it can be observed from the differential scanning calorimetry (DSC) thermograms in Fig. S2 of Supplementary Materials that upon heating, 10CN-COOH undergoes a crystal-to-smectic transition at 71.2  $^{\circ}$ C, then a smectic-to-nematic transition at 112.3  $^{\circ}$ C, and finally a nematic-to-isotropic transition at 121.9  $^{\circ}$ C, while during cooling it undergoes an isotropic-to-nematic transition at 106.7  $^{\circ}$ C, followed by a nematic-to-smectic transition at 93.9  $^{\circ}$ C and then a smectic-to-crystal transition at 47.1  $^{\circ}$ C.

### 3.2. Synthesis and structural characterizations of starch liquid crystalline polymer

Thereafter, 10CN-COOH was chlorinated by thionyl chloride and then reacted with starch in the medium of pyridine to give a thermotropic starch liquid crystalline polymer, denoted by St-10CN. This esterification approach was first reported by Mullen and Pacsu (1942). The rationale behind the use of pyridine as a solvent lies in that pyridine cannot only pre-activate the starch to open up the crystalline zone (amylase phase), improving the accessibility of esterifying reagent and ensuring more uniform substitution, but also perform as an efficient catalyst for acylation and an excellent acceptor for hydrochloric acid generated during the process of esterification.

Using Fourier transform infrared (FTIR) spectroscopy, we identified the chemical structures of St-10CN, as indicated in Fig. 1. For native starch (Fig. 1a), a strong broad absorption band appears at wavenumbers ranging from 3000 to 3600 cm<sup>-1</sup>, suggesting strong hydrogen bonding of hydroxyl groups in starch. This absorption band becomes negligibly small at a wavenumber of 3525 cm<sup>-1</sup> (Fig. 1c) after successful esterification of starch with mesogenic molecules, indicating that most of hydroxyl groups in starch have already been reacted. Further, this weak absorption peaks can be assigned to free -OH group, because the presence of hydrophobic mesogenic units largely interferes the hydrogen bonds between the residual hydroxyl groups. In Fig. 1b, the absorption peak at a wavenumber of 1697 cm<sup>-1</sup> characteristic of carboxylic acid (stretching of -OH group) for 10CN-COOH has completely shifted to 1737 cm<sup>-1</sup> in Fig. 1c, suggestive of the existence of carbonyl group in St-10CN.

Qualitatively, we have shown above using FTIR spectra that chemical modification decreased the total number of hydroxyl groups in the starch molecules, which has been replaced by mesogenic units. However, the number of hydroxyl groups substituted by mesogenic molecules and the number of hydroxyl groups available in a starch must be quantitatively determined. More often than not, the values of degree of substitution (DS) ranging from 0 to 3 are employed to define the number of hydroxyl groups substituted in each repeat unit of a starch (Aburto et al., 1997; Grote & Heinze, 2005; Neumann et al., 2002; Thiebaud et al., 1997). The DS of St-10CN was determined from its elemental analysis (C 74.65%, H 7.21%, O 14.82%, and N 3.32%). Assume that the degree of substitution of St-10CN is  $x$ , the percentage of nitrogen element can be expressed as the following Eq. (1), based on the number of elements in each repeated unit of St-10CN:

$$N\% = \frac{xN}{\underbrace{6C + 7H + 5O + (3-x)H}_{\text{Glucose unit}} + \underbrace{x(24C + 28H + 2O + N)}_{\text{mesogenic unit}}} \times 100\% \quad (1)$$

where C, H, O, and N represent carbon, hydrogen, oxygen and nitrogen elements, respectively. Substitution of the molecular weight of each element into Eq. (1) gives:

$$N\% = \frac{14.00674x}{162.1406 + 361.46592x} \times 100\% \quad (2)$$

Since  $N\% = 3.32\%$  obtained from elemental analysis, solving Eq. (2) gives  $x = 2.68$ . Therefore, the DS of St-10CN was calculated to be 2.68. Because of the high degree of substitution by mesogens, St-10CN is very hydrophobic and not soluble in water or dimethyl-sulfoxide. Instead, it can only dissolve in less polar solvents like chloroform and dichloromethane.

The chemical structure of St-10CN is further confirmed by proton NMR spectra present in Fig. 2. In the case of native starch (Fig. 2a), the chemical shifts at 5.50, 5.40, and 4.60 ppm are assigned to the protons of three hydroxyl groups at  $\alpha$ ,  $\beta$ , and  $\gamma$  positions in each repeated unit of starch, respectively. The chemical shift at 5.10 ppm is assigned to proton at C1 position, while the broad chemical shifts between 3.11 and 3.88 ppm are referred to as the proton at C2, C3, C4, C5, and C6 positions in every glucose unit. In Fig. 2b, the assignments of each peak for 10CN-COOH were given in Table 1. For St-10CN (Fig. 2c), the chemical shifts at 1.27, 1.73, and 2.34 ppm are assigned to proton of  $-\text{CH}_2-$  groups in mesogenic units, while the broad chemical shift at 3.89 ppm includes protons of  $-\text{CH}_2\text{O}-$  groups in mesogenic units as well as protons of C2–C6 in glucose unit. The chemical shifts between 4.0 and 5.5 ppm shows the protons of C1 in glucose unit and residual hydroxyl groups. It is obvious that the proton peaks of residual hydroxyl groups are very small as compared with those given in Fig. 2a. The protons of aromatic groups in mesogenic units reside at chemical shifts of 6.89 and 7.55 ppm. It can be distinguished from Fig. 2c that the chemical shift at 11.95 ppm (Fig. 2b), which is assigned to carboxylic acid group in 10CN-COOH, completely disappears. These observations are well consistent with the results obtained from FTIR spectra and elemental analysis, suggesting that the mesogenic molecules have been successfully attached onto the glucose unit of starch to a large extent.

### 3.3. Phase transitions, thermal stability and liquid crystalline behaviors of starch liquid crystalline polymers

Fig. 3 gives the DSC thermograms of St-10CN during the heating and cooling cycles at a scanning rate of  $10^\circ\text{C}/\text{min}$ . It is interesting to observe from Fig. 3 that St-10CN undergoes a glass transition temperature ( $T_g$ ) of  $29.6^\circ\text{C}$  and a clearing temperature ( $T_c$ ) of  $148.2^\circ\text{C}$  during heating, while it has a  $T_g$  of  $16.4^\circ\text{C}$  and  $T_c$  of

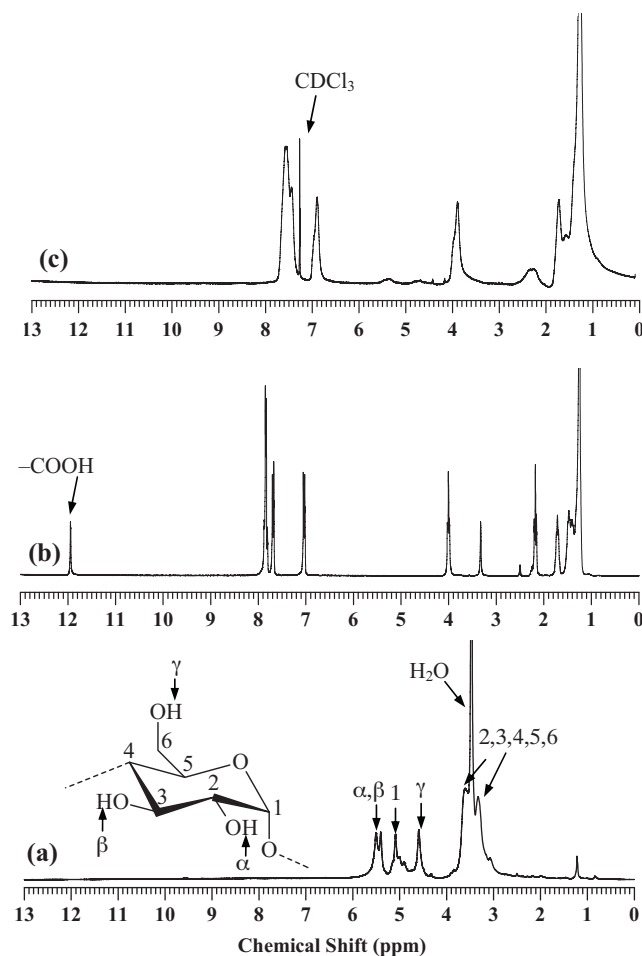


Fig. 2.  $^1\text{H}$  NMR spectra of (a) starch in DMSO, (b) 10CN-COOH in DMSO, and (c) starch-10CN in  $\text{CDCl}_3$ .

$142.5^\circ\text{C}$  upon cooling. Fig. 4 gives POM images of St-10CN during heating from  $130$  to  $160^\circ\text{C}$ , during which smectic mesophase gradually disappears, and upon cooling from the isotropic state, smectic mesophase re-appears. This demonstrates that St-10CN exhibits a smectic mesophase at the temperatures between  $29.6^\circ\text{C}$  and  $148.2^\circ\text{C}$ , and thus  $148.2^\circ\text{C}$  represents smectic-to-isotropic

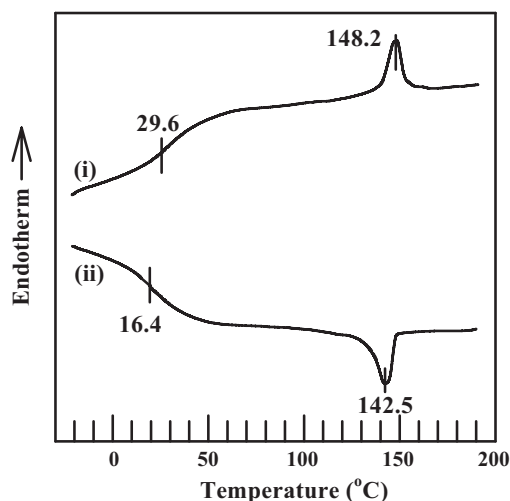


Fig. 3. (a) DSC thermograms of St-10CN during (i) heating and (ii) cooling cycles at a scanning rate of  $10^\circ\text{C}/\text{min}$ .



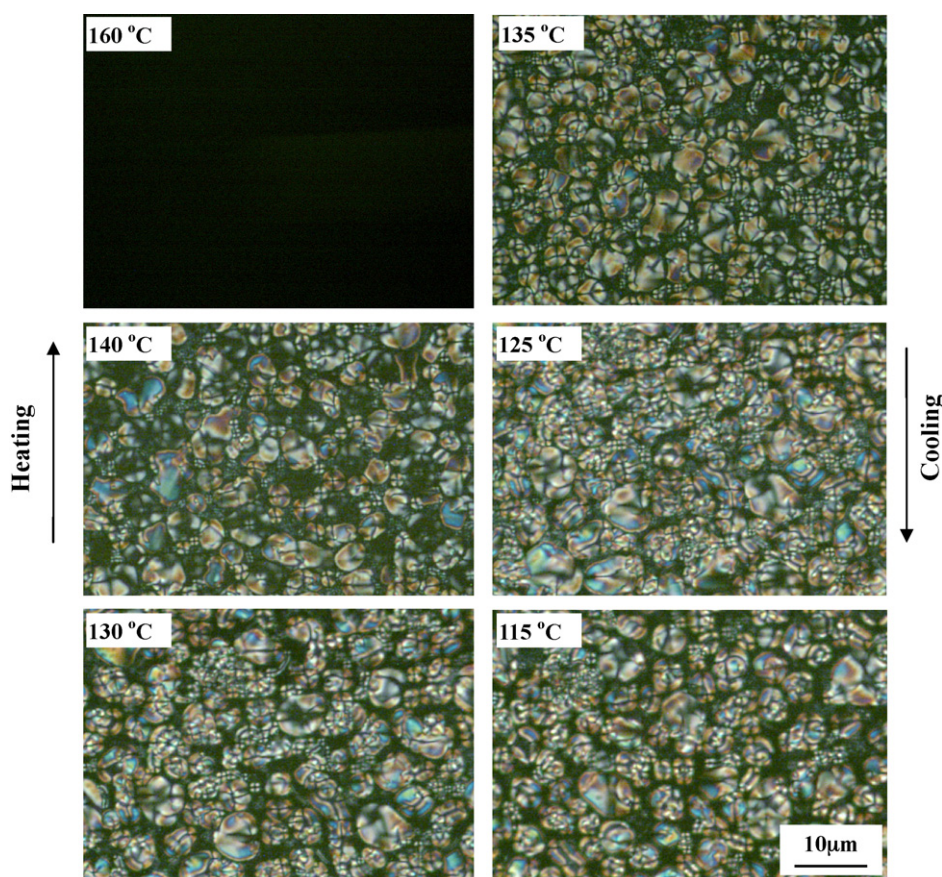


Fig. 4. POM images of St-10CN taken at different temperatures during the heating and cooling cycles.

(S-I) transition temperature ( $T_{SI}$ ). The high degree of substitution of hydroxyl groups in starch with mesogens results in the loss of crystallinity in the initially crystalline starch, and in turn St-10CN is a glassy smectic polymer. Moreover, it can be learned from thermogravimetric analysis present in Fig. S3 in the Supplementary Materials that the degradation temperature of St-10CN is above 300 °C, which is much higher than its  $T_{SI}$ . As compared with native starch, St-10CN has greater thermal stability, which is ascribable to the low concentration of hydroxyl groups in St-10CN and the high thermal stability of mesogenic units. The beneficial effects of good thermal stability would be easy processing (e.g. extrusion or injection molding) and the stability of final products for long-term applications.

The mesophase of St-10CN was also investigated by wide-angle X-ray diffraction (WAXD), as shown in Fig. 5. There exhibits a strong reflection peak at  $2\theta = \text{ca. } 20.1^\circ$  ( $d = 4.41 \text{ \AA}$ ), which corresponds to the outer diffuse halo in the WAXD pattern image given in the inset of Fig. 5, and is due to the distance between planes on which the oriented mesogenic groups lies. Another Bragg reflection peak at  $2\theta = \text{ca. } 5.35^\circ$  ( $d = 16.5 \text{ \AA}$ ) corresponds to the sharp inner ring in the WAXD pattern image, which is attributable to the pilling of layers. Thus, St-10CN has a smectic mesophase, which is in accordance with the observation of POM images present in Fig. 4. For side-chain liquid crystalline polymers, the length of flexible spacer in the side chain determines the mesophases of the polymers. If the number ( $n$ ) of methylene units is less than 6, nematic mesophase often occurs, whereas smectic mesophase dominates if  $n > 6$  (Akiyama, Nagase, Koide, & Araki, 1999; Lee & Han, 2003; Wewerka, Viertel, Vlassopoulos, & Stelzer, 2001). Since St-10CN may be considered as a side-chain liquid crystalline polymer with  $n > 6$ , it exhibits smectic mesophase, as expected.

### 3.4. Mechanical properties of starch liquid crystalline polymers

The tensile strengths for octanoated starch and dodecanoated starch with a degree of substitution of 2.7 were reported to be only 0.61 and 0.65 MPa, respectively, which were due to the fact that the fatty esters would have an effect of the internal plasticization on starch as well as cause the loss of crystallinity of starch molecules (Aburto et al., 1997; Thiebaud et al., 1997). The rather poor tensile strengths of these esterified starches made them difficult for practical applications and thus low density

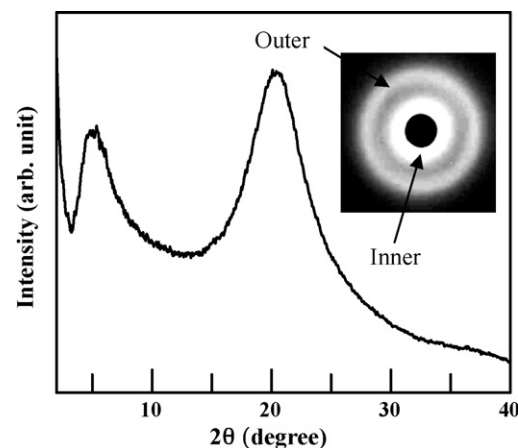


Fig. 5. Variation of X-ray diffraction intensity with scattering angle  $2\theta$  for St-10CN, which was annealed at 120 °C for 30 min and quenched in liquid nitrogen. The inset is its WAXD pattern image.

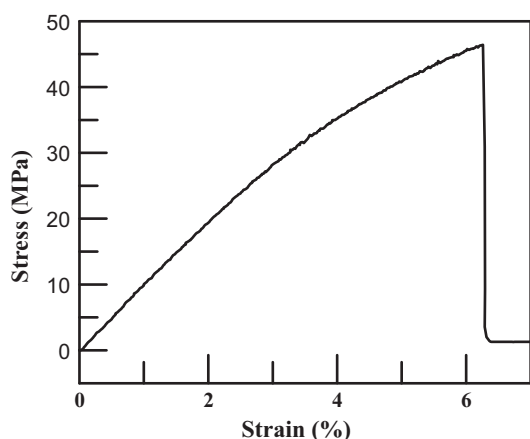


Fig. 6. Stress–strain curve for St-10CN.

Table 2

Mechanical properties of starch-based liquid crystalline polymer.

Tensile strength (MPa)	Tensile modulus (GPa)	Elongation at break (%)
37.9 ± 7.0	1.42 ± 0.14	6.09 ± 0.11

polyethylene was added to enhance their mechanical properties (Thiebaud et al., 1997). In contrast, the presence of mesogenic units in St-10CN facilitated the orientation of starch molecules. As a result, the mechanical properties of St-10CN were much higher than those of starch esters reported in the literature. Fig. 6 gives the stress–strain curve for St-10CN, indicating the highest tensile strength at break of 46.4 MPa among all the specimens measured. The average tensile strength for St-10CN is  $37.9 \pm 7.0$  MPa while its Young's modulus is  $1.42 \pm 0.14$  GPa, as indicated in Table 2. Nevertheless, the elongation at break is only  $6.09 \pm 0.11\%$ , which may be attributed to the rigid chains of both mesogenic side chains and starch molecules.

#### 4. Conclusion

To summarize, we have demonstrated an effective approach to functionalize starch with mesogens, the chemical structure of which was confirmed by FTIR and  $^1\text{H}$  NMR spectra. The degree of substitution of the resulted polymer was determined by elemental analysis to be 2.68. The phase transitions and liquid crystalline behaviors of this polymer were investigated by DSC, POM, and WAXD. St-10CN exhibits a glass transition temperature of  $29.6^\circ\text{C}$  and smectic-to-isotropic temperature of  $148.2^\circ\text{C}$  during the heating cycle, both of which are much lower than its thermal degradation temperature (above  $300^\circ\text{C}$ ). The tensile strength and Young's modulus of St-10CN were measured to be  $37.9 \pm 7.0$  MPa and  $1.42 \pm 0.14$  GPa. The successful synthesis of this unique thermotropic liquid crystalline polymer may open a new avenue for the engineering applications of starch.

#### Acknowledgements

Er Shi acknowledges the financial support from Research Foundations of Department of Science & Technology and Department of Education of Hunan Province, China. (Grant No. 2008SK4025 and 08 C114).

#### Appendix A. Supplementary data

Supplementary data associated with this article can be found, in the online version, at <http://dx.doi.org/10.1016/j.carbpol.2012.05.100>.

#### References

- Aburto, J., Alric, I., Thiebaud, S., Borredon, E., Bikiaris, D., Prinos, J., et al. (1999). Synthesis, characterization, and biodegradability of fatty-acid esters of amylose and starch. *Journal of Applied Polymer Science*, 74, 1440–1451.
- Aburto, J., Thiebaud, S., Alric, I., Borredon, E., Bikiaris, D., Prinos, J., et al. (1997). Properties of octanoated starch and its blends with polyethylene. *Carbohydrate Polymers*, 34, 101–112.
- Akiyama, E., Nagase, Y., Koide, N., & Araki, K. (1999). New side chain liquid crystalline polymers: Synthesis and thermal properties of side chain polyacrylates having segmented spacers. *Liquid Crystals*, 26, 1029–1037.
- Carvalho, A. J. F. (2008). Starch: Major sources, properties and applications as thermoplastic materials. In M. N. Belgacem, & A. Gandini (Eds.), *Monomers, polymers and composites from renewable resources* (pp. 321–342).
- Chen, J., Huang, Y., Yuan, J., Yan, S., & Ye, H. (1992). Thermotropic liquid crystalline behaviors of ethylcellulose. *Journal of Applied Polymer Science*, 45, 2153–2158.
- Choi, E.-J., Kim, C.-H., & Park, J.-K. (1999). Synthesis and characterization of starch-g-polycaprolactone copolymer. *Macromolecules*, 32, 7402–7408.
- Daniels, D. R., & Donald, A. M. (2004). Soft material characterization of the lamellar properties of starch: Smectic side-chain liquid-crystalline polymeric approach. *Macromolecules*, 37, 1312–1318.
- Donald, A. M., & Windle, A. H. (1992). In A. M. Donald, & A. H. Windle (Eds.), *Liquid crystalline polymers*. Cambridge: University Press.
- Dubois, P., Krishnan, M., & Narayan, R. (1999). Aliphatic polyester-grafted starch-like polysaccharides by ring-opening polymerization. *Polymer*, 40, 3091–3100.
- Greer, D. (2006). Plastic from plants, not petroleum. *BioCycle*, 47, 43–45.
- Grote, C., & Heinze, T. (2005). Starch derivatives of high degree of functionalization 11: Studies on alternative acylation of starch with long chain fatty acids homogeneously in N,N-dimethylacetamide/LiCl. *Cellulose*, 12, 435–444.
- Hu, T., Yi, J., Xiao, J., & Zhang, H. (2010). Effect of flexible spacer length on the mesophase structures of main-chain/side-chain liquid crystalline polymers based on ethyl cellulose. *Polymer Journal*, 42, 752–758.
- Huber, A. E., Kaplan, D. L., & Viney, C. (1994). Liquid crystallinity of levan/water/starch solutions. *Journal of Environmental Polymer Degradation*, 2, 195–199.
- Israelashvili, S. (1950). Mechanism of the nitration of starch. *Nature*, 165, 686–687.
- Lee, K. M., & Han, C. D. (2003). Effect of flexible spacer length on the rheology of side chain liquid crystalline polymers. *Macromolecules*, 36, 8796–8810.
- Liu, H., Xie, F., Yu, L., Chen, L., & Li, L. (2009). Thermal processing of starch-based polymers. *Progress in Polymer Science*, 34, 1348–1368.
- Mullen, J. W., & Pacsu, E. (1942). Preparation and properties of starch triesters. *Industrial & Engineering Chemistry*, 34, 1209–1217.
- Neumann, U., Wiege, B., & Warwel, S. (2002). Synthesis of hydrophobic starch esters by reaction of starch with various carboxylic acid imidazolides. *Starch/Stärke*, 54, 449–453.
- Petzold, K., Klemm, D., Stein, A., & Günther, W. (2002). Synthesis and NMR characterization of regiocontrolled starch alkyl ethers. *Designed Monomers & Polymers*, 5, 415–426.
- Shaikh, A. V. E., Maldar, N. N., Lonikar, S. V., Rajan, C. R., & Ponrathnam, S. (1999). Thermotropic liquid crystalline behavior of cholesterol-linked hydroxyethylcellulose. *Journal of Applied Polymer Science*, 72, 763–770.
- Thiebaud, S., Aburto, J., Alric, I., Borredon, E., Bikiaris, D., Prinos, J., et al. (1997). Properties of fatty-acid esters of starch and their blends with LDPE. *Journal of Applied Polymer Science*, 65, 705–721.
- Tomasik, P., & Schilling, C. H. (2004). Chemical modification of starch. *Advances in Carbohydrate Chemistry and Biochemistry*, 59, 175–403.
- Trimnell, D., Stout, E. I., Doane, W. M., & Russell, C. R. (1978). Preparation of starch 2-hydroxy-3-mercaptopropyl ethers and their use in graft polymerization. *Journal of Applied Polymer Science*, 22, 3579–3586.
- Waigh, T. A., Gidley, M. J., Komanshek, B. U., & Donald, A. M. (2000). The phase transformations in starch during gelatinisation: A liquid crystalline approach. *Carbohydrate Research*, 328, 165–176.
- Waigh, T. A., Kato, K. L., Donald, A. M., Gidley, M. J., Clarke, C. J., & Riekell, C. (2000). Side-chain liquid crystalline model for starch. *Starch/Stärke*, 52, 450–460.
- Waigh, T. A., Perry, P., Riekell, C., Gidley, M. J., & Donald, A. M. (1998). Chiral side-chain liquid crystalline polymeric properties of starch. *Macromolecules*, 31, 7980–7984.
- Werbosky, R. S., & Gray, D. G. (1976). Liquid crystalline structure in aqueous hydroxypropyl cellulose solution. *Molecular Crystals & Liquid Crystals*, 34, 97–103.
- Wewerka, A., Viertler, K., Vlassopoulos, D., & Stelzer, F. (2001). Structure and rheology of model side-chain liquid crystalline polymers with varying mesogen length. *Rheologica Acta*, 40, 416–425.
- Yang, B. Y., & Montgomery, R. (2006). Acylation of starch using trifluoroacetic anhydride promotor. *Starch/Stärke*, 58, 520–526.